JURNAL GEOGRAFI
Media Pengembangan Ilmu dan Profesi Kegeografian
http://journal.unnes.ac.id/sju/index.php/ujet

HIGH RISE BUILDING IDENTIFICATION FROM SPOT 6 MULTISPECTRAL AND DIGITAL SURFACE MODEL (DSM) USING OBJECT BASED IMAGE ANALYSIS

Zylshal, Zylshal[1]; Tejo Nugroho, Jalu[1]; Prasasti, Indah[1]
[1]Remote Sensing Application Center, Indonesian National Institute of Aeronautics and Space (LAPAN), Jl. Kalisari No. 8, Pekayon, Pasar Rebo, Jakarta Timur, Indonesia

Info Artikel

Keywords: *High-rise Building, SPOT-6, OBIA, DSM, Urban Geometry*

Abstract

This study focuses on one aspect of urban geometry called urban canyon. Urban canyon defined by a relatively narrow street lined by tall buildings. The initial step to extract the urban canyon is to identify the tall buildings. This study aims to discuss the potential use of the SPOT-6 multispectral data and its digital surface model (DSM), using object-based image analysis methods and terrain analysis, to identify the high-rise buildings in some part of Jakarta, Indonesia. Using slope and elevation percentile from the DSM as well as the spectral information of the SPOT-6 image, we then processed using the Object Image Analysis (OBIA) method and decision tree algorithm (crisp classification), we are able to obtained the identification rate of 78% with mean location accuracy of 30 meter (5 pixels).

✉ **Alamat korespondensi: Zylshal@lapan.go.id**

1. INTRODUCTION

The rapidly increasing growth of urban areas as well as the availability of high resolution/Very-High Resolution (VHR) imagery (Benediktsson *et al.,* 2012) make the urban related researches, spesifically building extraction topics, are increasing as well. Extracting building information on urban area via satellite images is not a new thing. Some previous research results show that the use of remote sensing data, in fact, is one of effective method to extract building information in urban area. Fraser *et al.* (2002) and (Liu *et al.,* 2005) used Quickbird with OBIA method coupled with PPHT (Progressive Probabilistic Hough Transformation) to extract square-shaped building with a roof. Slightly different approach, Sirmacek and Unsalan (2010) used a statistical analysis on the panchromatic aerial photographs and satellite imagery IKONOS, to conduct urban areas delineation in general. Shaker *et al.* (2011) used IKONOS stereo imagery on urban building extraction, and explained that it needed additional data, particularly related to the three-dimensional (3D) information.

The advancement of LiDAR (Light Detection and Ranging) technology, then opens up many possibilities and increases the amount of research related to the urban buildings extraction even further. Brédif *et al.* (2013) and Belgiu *et al.,* (2014) created a new approach on extracting building footprint using DSM data derived from LiDAR. Prerna and Singh (2015) compared the extraction method between the LiDAR data and aerial photograph; and found that the use of LiDAR data gives better results. Tomljenovic *et al.*, (2015) comprehensively analyzed various approaches that exist on urban buildings extraction with ALS (Airborne Laser Scanning) data. Their results show that it requires additional spectral information from aerial photograph or satellite image in order to give better results. These then emphasize the fact that combining both elevation information as well as spectral information can be used to increase the accuracy of building extraction in general. However, the use of LiDAR data, especially in Indonesia, is still not evenly distributed and relatively more expensive (Amin, 2015). For this reason, the photogrammetrically-derived DSM from stereo images may perform as a cost-effective data for urban buildings extraction.

The above explanation showed that in general, sub-meter VHR imagery is the best option to perform building extraction in urban areas. The problem is, specifically in Indonesia, that this type of data is only available in some big cities. VHR data such as Pleiades is currently available to selected government institutions (LAPAN, 2014) for a few cities in Indonesia. On the other hand, SPOT 6 data already covered almost all regions in Indonesia, specifically in provincial cities. SPOT-6 capability to record stereo/tri-stereo imagery (Bernard *et al.*, 2013) became one of the advantages that can be used to build DSM. Although it has 6 meter spatial resolution, the data is relatively much more coarse compared to the DSM built from VHR. Therefore, this study does not address the use of SPOT-6 data up to the level of building footprint, but only to the identification of tall buildings (high-rise building) in urban areas. Identifying these high-rise buildings is the first step towards monitoring urban heat island phenomenon, as it is directly connected to urban geometry (Ando *et al.*, 2009), especially regarding urban canyon (Battista *et al.*, 2015).

In this study, the urban features such as buildings, vegetation and river were regarded as a unified landscape. This approach opens the possibility of using terrain analysis methods which are commonly used in the field of geomorphology (Gerçek *et al.*, 2011; Huggett & Cheesman, 2002; Zylshal *et al.*,

2013) to be applied. High-rise buildings in this study were defined as any structures with 10 or more floors or with a minimum height of 20 meters (Craighead, 2009; Pandya & Brotas, 2014). This study was part of the more complete landuse/landcover mapping in Jakarta Region using SPOT-6 data conducted by (Zylshal *et al.*, 2015). This study in particular, focused on high-rise building identification and evaluates the accuracy. Recently, specific research on high-rise building identification using SPOT-6 in Jakarta, has never been done before.

2. METHODS

The test site for this study is a subset of SPOT-6 in Jakarta. The test area mainly focused on Sudirman area. This is one of Jakarta's central business district (Figure 1) located at Central Jakarta region.

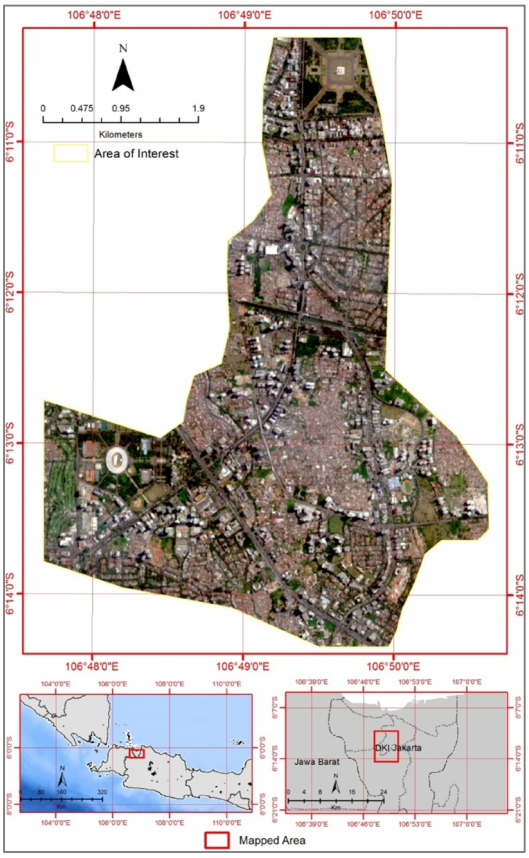

Figure 1. SPOT-6 data in true color composite showing the testing site at Central Jakarta Area

This area selected for its high profile office buildings and its contrast to residential building surrounds them. This characteristic deemed ideal to test the proposed method. The total testing area is 20.17 km^2. Landuse/landcover of the area generally dominated by dense residential and office space in the form of high-rise buildings, typical of urban areas. Some parts covered with vegetation such as trees, grass, and shrubs.

2.1 Data

This study used SPOT-6 Multispectral Orthorectified image, acquired at 27 August 2013, and SPOT-6 DSM built from stereo images. This study also used topographic map at 1:25.000 scale with contour interval at 12.5 meters as ancillary data. The SPOT-6 data specification is shown in Table 1.

This study used the 6 meter multispectral bands of SPOT-6 despite the fact that it has a panchromatic band with a higher resolution at 1.5 meters. The reason was that the pan-sharpening process will reduce the spectral quality of the image (Wald *et al.*, 1997). Another reason was that the object of interest on this study in the form of high-rise building is considered large enough to be represented by the multispectral bands. Since the DSM was also generated from the multispectral bands, it is appropriate to use the same level of spatial resolution for spectral information.

Table 1. Spesifikasi citra SPOT-6

Acquisition Time		**27 August 2013**
Spectral Range	Blue	0.455 µm – 0.525 µm
	Green	0.530 µm – 0.590 µm
	Red	0.625 µm – 0.695 µm
	Near Infrared	0.760 µm – 0.890 µm
Spatial Resolution	Panchromatic	1.5 m

Multispectral	6.0 m
Imaging Swath	60 km (Nadir)

Source: Airbus DS, 2012

2.2 Preprocessing

Before the data went into the segmentation and classification process, the SPOT-6 data needs to undergone a preprocessing step. Top of atmosphere (TOA) correction followed by Bidirectional Reflectance Distribution Function (BRDF) analysis were then performed. Elevation information obtained either from SPOT-6 DSM and topographic maps also should be preprocessed. The contour data from topographic maps were extracted and analyzed using ANUDEM algorithm (Hutchinson *et al.*, 2009; 2011) to generate Digital Elevation Model (DEM) with 12.5 meter spatial resolution. The DSM and DEM were then combined to make normalized DSM (nDSM) (Turker & Koc-San, 2015). nDSM contains the information about surface elevation relative to the terrain. Two layers of Land Surface Parameters (LSP)/ Digital Terrain Model (DTM) were then derived from nDSM. These LSPs are slope (Zevenbergen & Thorne, 1987) and elevation percentile (EPE) (Wilson & Gallant, 2000).

2.3 Segmentation

The segmentation and classification parameters in this study conducted using expert-based trial & error (Blaschke & Hay, 2001; Burnett & Blaschke, 2003; Duro *et al.*, 2012; Myint *et al.*, 2011; Zylshal *et al.*, 2013) in eCognition® Developer environment (Trimble, 2007). For the segmentation stage, this study used two segmentation algorithms. The first was the multiresolution segmentation algorithm based on the Fractal Net Evolution Approach (Baatz & Schäpe, 2000), and the second algorithm was Spectral difference Segmentation (Trimble, 2014). The segmentation was done on multilevel hierarchy approach with three levels (Figure 2).

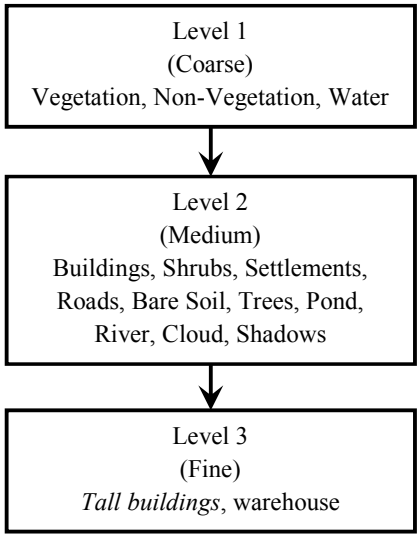

Figure 2. Segmentation and classification level hierarchy

For the multiresolution segmentation, we used the Estimation of Scale Parameters (ESP) tool (Drăguț *et al.*, 2010) to determine the optimum scale parameter. For the second algorithm we then only used the NDVI layer as an input on calculating the spectral difference between sub-objects.

After all the segmentation process was done, we then conducted a series of crisp classification based on threshold value. The classification scheme itself was built on an expert knowledge decision tree shown in Figure 3.

Most of the high-rise building in this study has a bright tone. This character were then identified and added as the distinguished features to further separate the high-rise building from other objects. The brightness value, calculated based on the equation 1 (Trimble, 2014).

$$\bar{c}(v) = \frac{1}{w^B} \sum_{k=1}^{K} w_k^B \, \bar{c}_k(v) \quad (1)$$

Where w_k^B was the brightness weight of image layer k with $w_k^B = \begin{cases} 0 \\ 1 \end{cases}$, K was the number of image layers k used for calculation, w^B is the sum of brightness weights of all image layers k used for

calculation with $w^B = \sum_{k=1}^{K} w_k^B$, $\bar{c}(v)$ was the mean instensity of image layer k of image object.

2.4 Accuracy Assessment

This study used two types of accuracy assessments. The first assessment was to measure the high rise identification accuracy of the proposed method. This assessment adapted from Jin and Davis (2005). Every high-rise building identified by the proposed method compared with the reference data, and divided into three categories. The three categories were: (a) true positive (TP) if the proposed method and reference data were both classified as "high-rise building", (b) false positive (FP) if only the proposed method classified as "high-rise building ", and (c) false negative (FN) if only the reference data that were classified as" high buildings ". After each object successfully defined into one of the three aforementioned categories, the identification accuracy were then calculated and presented in 3 kinds of information displayed in Table 2.

Table 2. Identification accuracy parameters for high-rise building object

Measurement	*Formula*
Branching Factor	$\frac{FP}{TP}$
Miss Factor	$\frac{FN}{TP}$
Detection Percentage	$100 \cdot \frac{TP}{TP + FN}$
Quality Percentage	$100 \cdot \frac{TP}{TP + FP + FN}$

Source: (Jin & Davis, 2005)

Detection percentage showed the correctly identified high-rise building by the proposed method. Branching factor calculate the commission error, and miss factor calculate the omission error. Quality percentage measured the absolute quality of high-rise building identification methodology proposed. This particular assessment, quoting (Jin & Davis, 2005) is the most "stringent measure". To have 100% value on quality percentage, the proposed method has to have the value of FN and FP equal to zero.

2.5 Location Accuracy

Location accuracy measurement in this study defined as the similarity between the classified object and the reference data location. The distance between the two objects was inversely proportional to the accuracy of its position. The smaller the distance between two objects, then higher its location accuracy value (Whiteside *et al.*, 2014). This study adopted the Loc measure from (Zhan *et al.*, 2005). The measurement was based on the Euclidean distance between the classified object and the reference data centroid.

$$Loc_{C_i,R_i} = \sqrt{\left(x_{C_i} - x_{R_i}\right)^2 + \left(y_{C_i} - y_{R_i}\right)^2} \quad (2)$$

where C_i is the evaluated object, R_i is the reference object, x_{C_i} and y_{C_i} are the centroid's coordinate of C, x_{R_i} and y_{R_i} are the centroid's coordinate of R.

Centroid coordinates for the classified object were then exported as point layer in GIS environment. Location accuracy was calculated by using Point Distance feature in Geospatial Modeling Environment Tool (GME) (Beyer, 2012). Summary statistics consisted of mean value, standard deviation, minimum, and maximum distances between two objects were then calculated. The complete data processing stages is shown in figure 3.

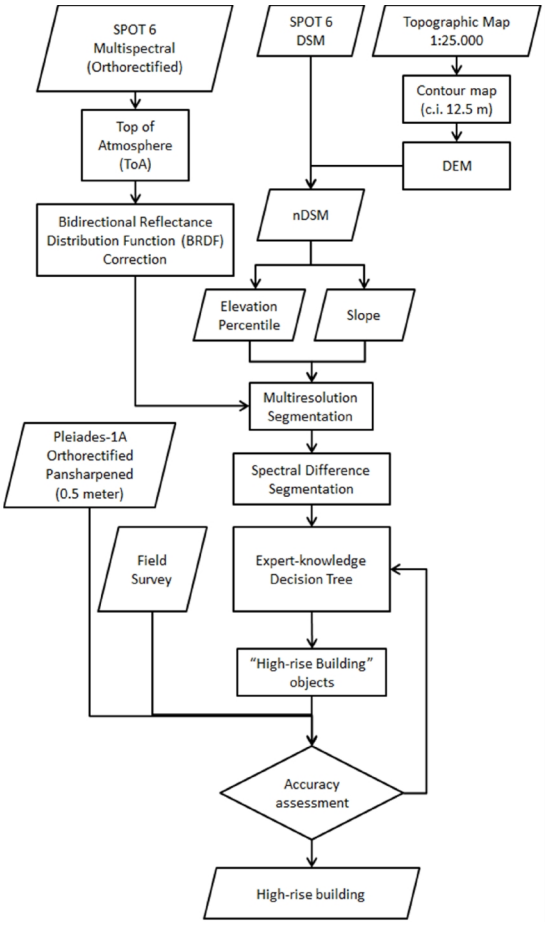

Figure 3. Data processing flowchart

3. RESULTS AND DISCUSSION

The ESP Tool results are shown in Figure 5. Four optimum scale parameters (79, 90, 116, and 156) were then chosen for the first segmentation stage. We then applied each scale parameters and visually evaluate the results as the most suitable for our research purposes.

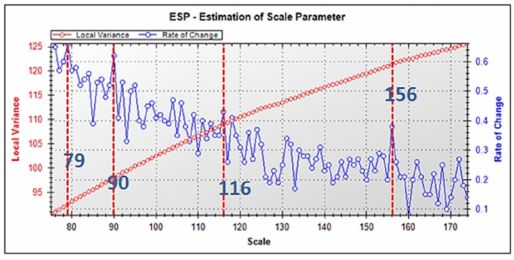

Figure 5. ESP tool result. The dotted line indicated some of the optimum scale parameters

We then decided to use 79 as the scale parameter for our study. Although the result tended to be over-segmented in some part of the image, the smaller object such as high-rise building rooftop can still be identified. This finding, is complied with Hay and Castilla (2008). For the relatively homogenous objects (i.e. lake, grass field) which still over-segmented, we then conducted a second segmentation stage using Spectral Difference Segmentation algorithm. The complete parameters value used in these segmentation stages is shown in Table 3.

Table 3. Segmentation Parameters

Level	Segmentation Algorithms	*Layers input*	*Scale*	*Shape*	*Compactness*
1	*Multiresolution Segmentation*	*Blue, Green, Red,* NIR	79	0.35	0.1
2	*Spectral Difference Segmentation*	NDVI	*Maximum Spectral Difference*		
			0.005		

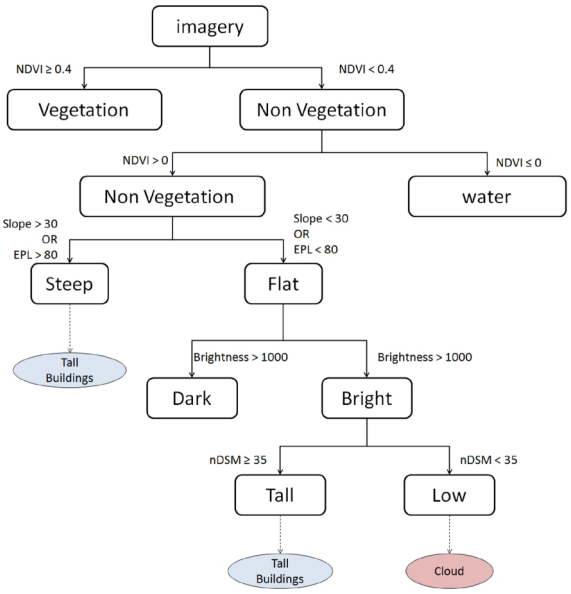

Figure 4. high rise building identification's decision tree

A set of decision tree ruleset were generated, as illustrated in Figure 4, to differentiate and extract tall buildings within the test site. Each branch was performed

using crisp classification with a specific threshold. The threshold value was determined using trial and error method.

Following the decision tree in Figure 4, we were able to extract 250 "high-rise buildings" objects. These objects were then compared with reference data for its location accuracy as well as the identification accuracy (Figure 6).

This study found that the detection percentage was at 78% with miss factor at 0.28. The assessment revealed that there are quite a lot of misclassified object, especially for the false positive identification. This then resulted in the high branching factor at 0.9 as well as the low quality percentage at 45.77%, as shown in Table 4.

Table 4. High-rise building identification accuracy

Identification Assessment	Values
No. Objects	250
TP	195
FP	176
FN	55
Branching Factor	0.90
Miss Factor	0.28
Detection Percentage (%)	78
Quality Percentage (%)	45.77

TP: True Positive, FP: False Positive, FN: False Negative

We managed to obtain 250 pairs of reference data and the classified object to calculate the location accuracy (Table 5). The average location difference for each object's centroid was at 12.74 meters (± 2 pixels) with a standard deviation ranged from 0 to 9.89 meters (1.6 pixels). The maximum location difference was at 49 meters (± 8 pixels), and the smallest was 0 meters. These finding was correspond to the (Astrium, 2014) technical sheet for SPOT-6/7 ortho products.

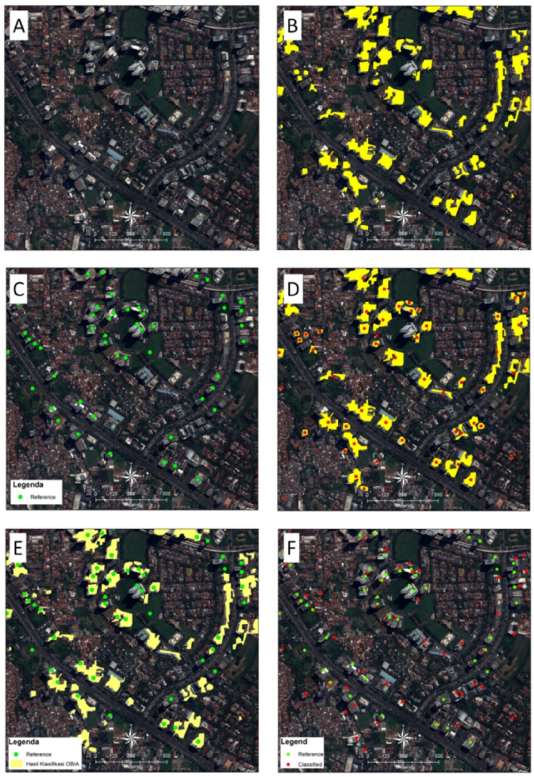

Figure 6. Subset Pleiades-1A RGB 321 (a) Before the segmentation, (b) Yellow polygon indicate the extracted "tall building" from OBIA method, (c) The reference points data identified from Pleiades-1A visual interpretation, (d) the polygon identified from OBIA and its respective point features (as indicated with red dot), (e) the identification accuracy assessment, (f) location accuracy assessment (Pleiades © 2012 Distribution Airbus DS)

The proposed identification method in this study was not able to provide the separation between adjacent high buildings as shown in Figure 7, due to its 6 meter spatial resolution, compared to the much higher resolution of Pleaides-1A image. For a complex of high-rise buildings, this was identified as a single object represented by the yellow polygon. As in the Pleiades-1A, it was visually clear how the towers are separated each other and can be identified as different high-rise buildings.

Table 5. Summary statistics of the Euclidean distance between the reference data and the classified objects

Statistik	Value
No. of object pairs	250
Mean Distance (*MeanLoc*)	12.74
Maximum	49.26
Minimum	0
Standar Deviasi (*StDevLoc*)	9.89

There are several reasons why the identification accuracy was only at 78%. First, it was by the fact that the high noise that exist in the DSM SPOT-6 data used in this study, as explained in (Zylshal *et al.*, 2015). This then created the false positive result, because these noises were creating false peak in the DSM, which then picked up by the classification algorithm as tall objects. The second reason was because we use contour map to build the DEM, which has a difference in spatial resolution as well as the vertical accuracy. Thus, preprocessing the DSM prior to segmentation and classification, as well as building DEM directly from SPOT-6 DSM needs to be done in order to minimize these errors. The use of higher resolution DSM data such as LiDAR or from the stereo image of VHR imagery such as Pleiades and Worldview-3 might give a better result since it will provide a better resolution (Bachofer & Hochschild, 2015; Brédif *et al.*, 2013; Jin & Davis, 2005; Nyaruhuma *et al.*, 2012; Pfeifer *et al.*, 2007; Sebari & He, 2013; Shaker *et al.*, 2011; Song *et al.*, 2015), but also it is needed to pointed out that these higher resolution data would also means a more detailed information, which is outside of this paper's original objective. Additional road network can also be used to eliminate the false positive even further by doing distance analysis, since typically, these high-rise building constructed near the main road, as it has been proven by (Duke *et al.*, 2003; Dupuy *et al.*, 2012; Hagenlocher *et al.*, 2012; Kontoes *et al.*, 1993).

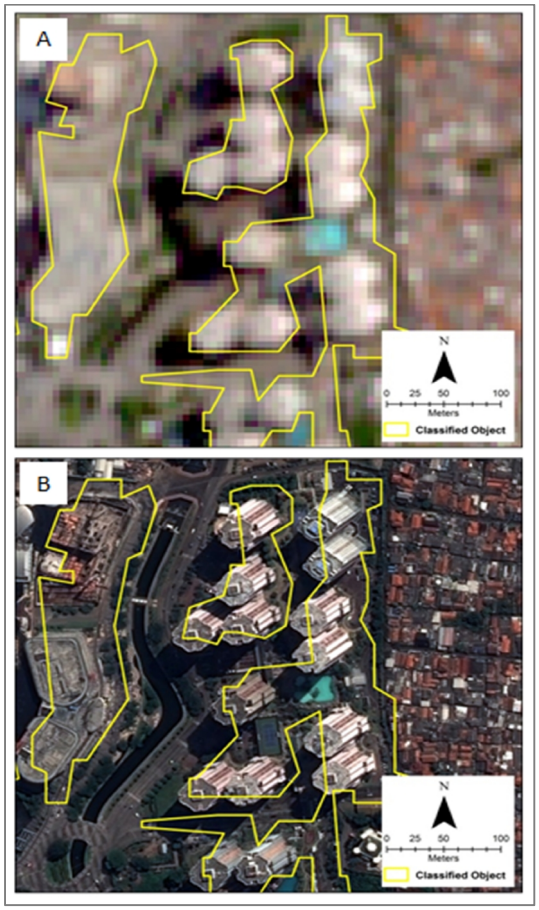

Figure 7. Comparison on high-rise building viewed from SPOT-6 and Pleiades-1A imagery (a) SPOT-6 RGB 321 with classified "tall building" overlaid on top with as yellow polygons, (b) Pleiades-1A RGB 321 with classified "tall building" overlaid on top with as yellow polygons (Pleiades © 2012 Distribution Airbus DS).

Even with the lack of separation between several "high-rise" buildings in some areas, considering its 6 meter spatial resolution, SPOT-6 data coupled with the proposed method used in this study, considered quite capable of providing an initial information regarding the area that can cause an urban canyon effect. It is emphasized that the proposed method was tied to the specific data and area used in this study. How the method performs in other data, or other areas still need to be studied

further to see the consistency. Even so, the workflows and algorithms in this study could still be used for the identification of high-rise building in other areas, by making modifications to the parameters of the existing segmentation and classification in accordance with the characteristics of the region.

4. CONCLUSION

This study proposed terrain analysis approach on urban study using OBIA method and photogrammetrically-derived DSM from SPOT-6 satellite data and found that the detection percentage rate was 78%. The proposed method in this study indicates a large potential of SPOT-6 data, especially with its ability to provide stereo imagery to be used as an alternative method on tall buildings identification in urban areas. With its 6 meter spatial resolution on multispectral band, SPOT-6 can still be used for urban area, as this study shown. The identification results can be used as an initial step towards understanding and monitoring the urban geometry and urban canyon as one of the factors that influence the urban heat island phenomenon. One of the strong points on this study is that, by using the same source (i.e. SPOT-6) on spectral and elevation information, it can produce good results in terms of location accuracy. Since the study focused on building identification rather that building footprint extraction, the location accuracy becomes more important. For further research, the use of higher spatial resolution such as the Pansharpened SPOT-6 imagery, with 1.5 meter spatial resolution should be investigated. It is also recommended to see how the proposed method performs on the VHR data with stereo/tristereo recording capability such as WorldView-3 and Pleiades. Additional vector data can also be used to improve the accuracy of identification results. These options are part of our future research.

The authors would like to thank LAPAN Remote Sensing Technology and Data Center for the provision of SPOT-6 images, both its multispectral and DSM data. The authors also would like to acknowledge the Environment research team of Environmental and Disaster Mitigation division, Remote Sensing Application Center for their contribution on field data collection used in this study.

5. REFERENCES

Amin, M. B. Al. (2015). Pemanfaatan Teknologi Lidar Dalam Analisis Genangan Banjir Akibat Luapan Sungai Berdasarkan Simulasi Model Hidrodinamik. *Info Teknik*, *16*(1), 21–32.

Ando, H., Morishima, W., Yokoyama, H., & Akasaka, I. (2009). Effects of Urban Geometry on Urban Heat Islands in Tokyo. In *The Seventh International Conference on Urban Climate* (p. 4). Yokohama, Japan.

Astrium. (2014). SPOT 6/SPOT 7 Technical Sheet, 1–4.

Bachofer, F., & Hochschild, V. (2015). A SVM-based Approach to Extract Building Footprints from Pléiades Satellite Imagery. In *Geotech Rwanda 2015* (pp. 1–4). Kigali, Rwanda.

Battista, G., Evangelisti, L., Guattari, C., & Vollaro, R. D. L. (2015). On the Influence of Geometrical Features and Wind Direction over an Urban Canyon Applying a FEM Analysis. *Energy Procedia*, *81*, 11–21. https://doi.org/10.1016/j.egypro.2015.12.054

Belgiu, M., Dragut, L., & Strobl, J. (2014). Quantitative evaluation of variations in rule-based classifications of land cover in urban neighbourhoods using WorldView-2 imagery. *ISPRS Journal of Photogrammetry and Remote Sensing*, *87*, 205–215. https://doi.org/10.1016/j.isprsjprs.2013.11.007

Benediktsson, J. A., Chanussot, J., & Moon, W. M. (2012). Very high-resolution remote sensing: challenges and opportunities. *Proceedings of the*

IEEE, *100*(6), 1907–1910. https://doi.org/10.1109/JPROC.2012.2190811

Bernard, M., Decluseau, D., Gabet, L., & Nonin, P. (2013). *3D Capabilities of Spot 6*. Retrieved from http://www.intelligence-airbusds.com/files/pmedia/public/r28533_9_icc2013_3d_capabilities_of_spot_6.pdf

Beyer, H. L. (2012). Geospatial Modelling Environment. *Geospatial Modeling Environment*.

Blaschke, T., & Hay, G. J. (2001). Object-oriented image analysis and scale-space: theory and methods for modeling and evaluating multiscale landscape structure. *International Archives of Photogrammetry and Remote Sensing*, *34*(4), 22–29.

Brédif, M., Tournaire, O., Vallet, B., & Champion, N. (2013). Extracting polygonal building footprints from digital surface models: A fully-automatic global optimization framework. *ISPRS Journal of Photogrammetry and Remote Sensing*, *77*, 57–65. https://doi.org/10.1016/j.isprsjprs.2012.11.007

Burnett, C., & Blaschke, T. (2003). A multi-scale segmentation/object relationship modelling methodology for landscape analysis. *Ecological Modelling*, *168*(3), 233–249. https://doi.org/10.1016/S0304-3800(03)00139-X

Craighead, G. (2009). High-Rise Building Definition, Development, and Use. *High-Rise Security and Fire Life Safety (Third Edition)*, (August 2005), 1–26. https://doi.org/10.1016/B978-1-85617-555-5.00001-8

Drăguţ, L., Tiede, D., & Levick, S. R. (2010). ESP: a tool to estimate scale parameter for multiresolution image segmentation of remotely sensed data. *International Journal of Geographical Information Science*, *24*(6), 859–871. https://doi.org/10.1080/13658810903174803

Duke, G. D., Kienzle, S. W., Johnson, D. L., & Byrne, J. M. (2003). Improving overland flow routing by incorporating ancillary road data into Digital Elevation Models. *Journal of Spatial Hydrology*, *3*(2), 27.

Dupuy, S., Barbe, E., & Balestrat, M. (2012). An object-based image analysis method for monitoring land conversion by artificial sprawl use of RapidEye and IRS data. *Remote Sensing*, *4*(2), 404–423. https://doi.org/10.3390/rs4020404

Duro, D. C., Franklin, S. E., & Dube, M. G. (2012). A comparison of pixel-based and object-based image analysis with selected machine learning algorithms for the classification of agricultural landscapes using SPOT-5 HRG imagery. *Remote Sensing of Environment*, *118*, 259–272. https://doi.org/10.1016/j.rse.2011.11.020

Fraser, C. S., Baltsavias, E., & Gruen, A. (2002). Processing of Ikonos imagery for submetre 3D positioning and building extraction. *ISPRS Journal of Photogrammetry and Remote Sensing*, *56*(3), 177–194. https://doi.org/http://dx.doi.org/10.1016/S0924-2716(02)00045-X

Gerçek, D., Toprak, V., & Strobl, J. (2011). Object-based classification of landforms based on their local geometry and geomorphometric context. *International Journal of Geographical Information Science*, *25*(6), 1011–1023. https://doi.org/10.1080/13658816.2011.558845

Hagenlocher, M., Lang, S., & Tiede, D. (2012). Integrated assessment of the environmental impact of an IDP camp in Sudan based on very high resolution multi-temporal satellite imagery. *Remote Sensing of Environment*, *126*(August 2016), 27–38. https://doi.org/10.1016/j.rse.2012.08.010

Hay, G. J., & Castilla, G. (2008). Geographic Object-Based Image Analysis (GEOBIA): A new name for a new discipline. In T. Blaschke, S. Lang, & G. J. Hay (Eds.), *Object-Based Image Analysis: Spatial Concepts for Knowledge-Driven Remote Sensing Applications* (pp. 75–89). Berlin,

Heidelberg: Springer Berlin Heidelberg. https://doi.org/10.1007/978-3-540-77058-9_4

Huggett, R. J., & Cheesman, J. (2002). *Topography and the Environment*. Prentice Hall.

Hutchinson, M. F., Stein, J. A., Stein, J. L., & Xu, T. (2009). Locally adaptive gridding of noisy high resolution topographic data. *18th World IMACS Congress and MODSIM09 International Congress on Modelling and Simulation: Interfacing Modelling and Simulation with Mathematical and Computational Sciences, Proceedings*, (July), 2493–2499.

Hutchinson, M., Xu, T., & Stein, J. (2011). Recent Progress in the ANUDEM Elevation Gridding Procedure. In T. Hengel, I. S. Evans, J. P. Wilson, & M. Gould (Eds.), *Geomorphometry 2011* (pp. 19–22). Redlands, California.

Jin, X., & Davis, C. H. (2005). Automated Building Extraction from High-Resolution Satellite Imagery in Urban Areas Using Structural, Contextual, and Spectral Information. *EURASIP Journal on Advances in Signal Processing*, *2005*(14), 2196–2206. https://doi.org/10.1155/ASP.2005.2196

Kontoes, C., Wilkinson, G. G., Burrill, A., Goffredo, S., & Mégier, J. (1993). An experimental system for the integration of GIS data in knowledge-based image analysis for remote sensing of agriculture. *International Journal of Geographical Information Systems*, *7*(3), 247–262. https://doi.org/10.1080/02693799308901955

LAPAN. (2014). *The Remote Sensing Monitoring Program of Indonesia's National Carbon Accounting System: Methodology and Products, Version 1*. Jakarta, Indonesia.

Liu, Z. J., Wang, J., & Liu, W. P. (2005). Building extraction from high resolution imagery based on multi-scale object oriented classification and probabilistic Hough transform. In *Proceedings. 2005 IEEE International Geoscience and Remote Sensing Symposium, 2005. IGARSS '05.* (Vol. 4, pp. 2250–2253). IEEE. https://doi.org/10.1109/IGARSS.2005.1525421

Myint, S. W., Gober, P., Brazel, A., Grossman-Clarke, S., & Weng, Q. (2011). Per-pixel vs. object-based classification of urban land cover extraction using high spatial resolution imagery. *Remote Sensing of Environment*, *115*(5), 1145–1161. https://doi.org/10.1016/j.rse.2010.12.017

Nyaruhuma, A. P., Gerke, M., Vosselman, G., & Mtalo, E. G. (2012). Verification of 2D building outlines using oblique airborne images. *ISPRS Journal of Photogrammetry and Remote Sensing*, *71*, 62–75. https://doi.org/10.1016/j.isprsjprs.2012.04.007

Pandya, S. V, & Brotas, L. (2014). Tall Buildings and the Urban Microclimate in the City of London. In *30th International PLEA Conference* (pp. 1–8). CEPT University, Ahmedabad.

Pfeifer, N., Rutzinger, M., Rottensteiner, F., Muecke, W., & Hollaus, M. (2007). Extraction of building footprints from airborne laser scanning: Comparison and validation techniques. *2007 Urban Remote Sensing Joint Event, URS*. https://doi.org/10.1109/URS.2007.371854

Prerna, R., & Singh, C. K. (2015). Evaluation of LiDAR and image segmentation based classification techniques for automatic building footprint extraction for a segment of Atlantic County, New Jersey. *Geocarto International*, *6049*(October), 1–20. https://doi.org/10.1080/10106049.2015.1076060

Sebari, I., & He, D. C. (2013). Automatic fuzzy object-based analysis of VHSR images for urban objects extraction. *ISPRS Journal of Photogrammetry and Remote Sensing*, *79*, 171–184. https://doi.org/10.1016/j.isprsjprs.2013.02.006

Shaker, I. F., Abd-Elrahman, A., Abdel-Gawad, A. K., & Sherief, M. A. (2011). Building extraction from high resolution space images in high

density residential areas in the Great Cairo region. *Remote Sensing*, *3*(4), 781–791. https://doi.org/10.3390/rs3040781

Sirmacek, B., & Unsalan, C. (2010). Urban area detection using local feature points and spatial voting. *IEEE Geoscience and Remote Sensing Letters*, *7*(1), 146–150. https://doi.org/10.1109/LGRS.2009.2028744

Song, J., Wu, J., & Jiang, Y. (2015). Extraction and reconstruction of curved surface buildings by contour clustering using airborne LiDAR data. *Optik*, *126*(5), 513–521. https://doi.org/10.1016/j.ijleo.2015.01.011

Tomljenovic, I., Höfle, B., Tiede, D., & Blaschke, T. (2015). Building Extraction from Airborne Laser Scanning Data: An Analysis of the State of the Art. *Remote Sensing*, *7*(4), 3826–3862. https://doi.org/10.3390/rs70403826

Trimble. (2007). eCognition® Developer 7 reference book. *Definiens AG, München*, 21–24.

Trimble. (2014). *eCognition ® Developer Reference Book*. Trimble. Germany.

Turker, M., & Koc-San, D. (2015). Building extraction from high-resolution optical spaceborne images using the integration of support vector machine (SVM) classification, Hough transformation and perceptual grouping. *International Journal of Applied Earth Observation and Geoinformation*, *34*(1), 58–69. https://doi.org/10.1016/j.jag.2014.06.016

Wald, L., Ranchin, T., & Mangolini, M. (1997). Fusion of Satellite Images of Different Spatial Resolution: Assessing the Quality of Resulting Images. *Photogrammetric Engineering & Remote Sensing*, *63*(6), 691–699.

Whiteside, T. G., Maier, S. W., & Boggs, G. S. (2014). Area-based and location-based validation of classified image objects. *International Journal of Applied Earth Observation and Geoinformation*, *28*(1), 117–130. https://doi.org/10.1016/j.jag.2013.11.009

Wilson, J. P., & Gallant, J. C. (2000). *Terrain Analysis: Principles and Applications*. Wiley.

Zevenbergen, L. W., & Thorne, C. R. (1987). Quantitative analysis of land surface topography. *Earth Surf. Process. Landforms*. https://doi.org/10.1002/esp.3290120107

Zhan, Q., Molenaar, M., Tempfli, K., & Shi, W. (2005). Quality assessment for geo-spatial objects derived from remotely sensed data. *International Journal of Remote Sensing*, *26*(14), 2953–2974. https://doi.org/10.1080/01431160500057764

Zylshal, Danoedoro, P., & Haryono, E. (2013). An object based image analysis approach to semi-automated karst morphology extraction. *34th Asian Conference on Remote Sensing 2013, ACRS 2013*, *1*, 927–934. Retrieved from http://a-a-r-s.org/acrs/administrator/components/com_jresearch/files/publications/SC02-0308_Full_Paper_ACRS2013_Zylshal.pdf

Zylshal, Yulianto, F., Pasaribu, J. M. J. M., & Prasasti, I. (2015). Landuse / Landcover Extraction From Spot 6 Imagery Using Object Based Image Analysis Approach : a Case Study of Jakarta ,. In *Proceedings of ACRS 2015*. Quenzhon City, Metro Manila, Philippines.